J Mol Model (2018) 24: 157
https://doi.org/10.1007/s00894-018-3660-5

ORIGINAL PAPER

Chemical sensors based on N-substituted polyaniline derivatives: reactivity and adsorption studies via electronic structure calculations

Larissa O. Mandú[1] · **Augusto Batagin-Neto**[1]

Received: 6 February 2018 / Accepted: 13 April 2018 / Published online: 9 June 2018

Abstract

Conjugated organic polymers represent an important class of materials for varied technological applications including in active layers of chemical sensors. In this context, polyaniline (PANI) derivatives are promising candidates, mainly due to their high chemical stability, good processability, versatility of synthesis, polymerization, and doping, as well as relative low cost. In this study, electronic structure calculations were carried out for varied N-substituted PANI derivatives in order to investigate the potential sensory properties of these materials. The opto-electronic properties of nine distinct compounds were evaluated and discussed in terms of the employed substituents. Preliminary reactivity studies were performed in order to identify adsorption centers on the oligomer structures via condensed-to-atoms Fukui indexes (CAFI). Finally, adsorption studies were carried out for selected derivatives considering five distinct gaseous analytes. The influence of the analytes on the oligomer properties were investigated via the evaluation of average binding energies and changes on the structural features, optical absorption spectra, frontier orbitals distribution, and total density of states in relation to the isolated oligomers. The obtained results indicate the derivatives PANI-NO_2 and PANI-C_6H_5 as promising materials for the development of improved chemical sensors.

Keywords Chemical sensors · N-substituted polyaniline derivatives · Electronic structure calculations · Reactivity indexes · Adsorption study

Introduction

The monitoring and control of gaseous compounds are relevant activities in varied areas of the economy, such as industrial production, automobile industry, medical applications, air quality monitoring, and environmental studies [1, 2]. Such activities are usually carried out with the aid of chemical sensors.

Given their high sensitivity and short typical response times, conductive organic polymers have been considered as promising materials for applications in active layers of chemical sensors [3]. In this context, polyaniline (PANI) derivatives have been identified as very interesting candidates and they have already been successfully employed in this area [4–11]. This conjugated polymer presents a basic structure composed of a varied ratio of reduced (amines) and oxidized (imines) subunits that confers unique electrical properties to this material [12–14]. Besides their interesting opto-electronic properties, PANI derivatives also present high chemical stability, good processability, ease of polymerization/doping, and low relative cost, which enable their use in varied technological applications [15, 16].

Over the years, distinct PANI derivatives have been proposed in order to obtain materials with improved solubility and modified opto-electronic responses [17–19]. In this context, the incorporation of substituents into the PANI structure by N-substitution have proven to be an efficient approach to the production of soluble/processable derivatives with varied properties [19–28].

In these materials, the presence of side groups attached to the nitrogen atom of the PANI basic structure hinders the characteristic salt-base transition of the unmodified

This paper belongs to Topical Collection *XIX - Brazilian Symposium of Theoretical Chemistry (SBQT2017)*

Electronic supplementary material The online version of this article (https://doi.org/10.1007/s00894-018-3660-5) contains supplementary material, which is available to authorized users.

✉ Augusto Batagin-Neto
abatagin@itapeva.unesp.br

Larissa O. Mandú
larissa-mandu@hotmail.com

[1] São Paulo State University (UNESP), Campus of Itapeva, Itapeva, São Paulo, Brazil

polymer, leading to significant changes in the reactivity, stability, as well as in the opto-electronic properties of the compounds [27–29]. Given the profound influence of N–H bonds in the polymer properties, N-substituted PANI derivatives are particularly expected to present quite distinct responses to changes on the polymer environment, which can be interesting for applications in chemical sensors.

In this study, the opto-electronic properties and local reactivity of distinct N-substituted PANI derivatives were evaluated in order to identify new promising materials for applications in chemical sensors. The influence of the distinct side groups on the opto-electronic properties of the systems was firstly investigated. Pre-evaluations of the local reactivities were then carried out to select relevant systems for subsequent adsorption studies. Finally, details regarding analyte–polymer interactions as well as the influence of the analytes on the optoelectronic properties of the oligomers were investigated for the most promising systems. The results point out the derivatives PANI-NO_2 and PANI-C_6H_5 as interesting materials for the design of chemical sensors with improved responses.

Materials and methods

Figure 1 shows the basic units of N-substituted PANI derivatives considered in the present study (PANI-R). The **R** groups were chosen according to their Hammet indexes, which indicate the effect of the insertion of side groups on resonant systems [30]. In general, these indexes describe the tendency of a given substituent to insert (or remove) electrons in (of) a given resonant systems by inductive (σ_I) or resonant (σ_R) effects. Positive values of σ_X (for $X = R$ or I) suggest that the substituent acts as an electron-withdrawing group (EWG) while negative values are associated with electron-releasing groups (ERG). Table 1 shows the substituents employed and their Hammet parameters. Only neutral unmodified PANI (**R**=H, leucoemeraldine base) was employed in this study aiming to facilitate the comparison with the other systems.

Based on a preliminary study on the saturation of opto-electronic properties of the unmodified PANI, structures with ten units were considered for all the systems.

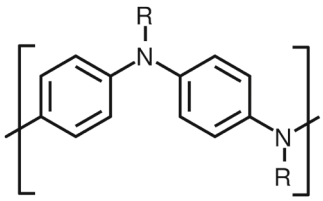

Fig. 1 Basic structure of the N-substituted PANI derivatives (PANI-R)

Table 1 N-substituents employed (see Fig. 1) and associated Hammet parameters for inductive (σ_I) and resonant effects (σ_R) [30]

ID	R	σ_I	σ_R
1	H	0	0
2	OH	0.24	−0.62
3	NO_2	0.67	0.1
4	C_6H_5	0.12	−0.11
5	$C(CH_3)_3$	−0.01	−0.18
6	NH_2	0.17	−0.8
7	CH_3	−0.01	−0.16
8	C≡CH	0.29	−0.04
9	F	0.54	−0.48

For reactivity study, isolated structures of the derivatives were fully optimized *in vacuo* in a Hartree–Fock (HF) approach, by using the PM6 semi-empirical method [31] implemented in the MOPAC2016 computational package [32, 33]. The choice of a semi-empirical method for geometry optimization was based on the number of distinct structures evaluated and their relative large size, aiming to minimize the computational cost. We do not consider that this approach is a severe limitation since a number of works show that a reasonable description of opto-electronic properties of similar systems can be obtained by considering geometries coming from semi-empirical calculations in conjunction more sophisticated *ab initio* or density functional theory (DFT)-based methods [34–36].

Local reactivities were evaluated via condensed-to-atoms Fukui indexes (CAFI) [37]. In an adiabatic approach, such descriptors indicate how the frontier orbitals are modified when small changes are performed on the number of electrons present in the system, and have been successfully employed in the study of molecules and polymers reactivities [38–42]. Given the way they are defined, it is possible to obtain three distinct CAFIs: f^+, f^-, and f^0, associated with local reactivities towards nucleophilic, electrophilic, or free-radical chemical species, respectively.

$$f_k^+ = q_k(N+1) - q_k(N) \quad (1)$$

$$f_k^- = q_k(N) - q_k(N-1) \quad (2)$$

$$f_k^0 = \frac{1}{2}\left[q_k(N+1) - q_k(N-1)\right] \quad (3)$$

where $q_k(N+1)$, $q_k(N)$, and $q_k(N-1)$ represent, respectively, the electronic populations on the k-th atom of the anionic, neutral, and cationic configurations of the system under study.

It is important to highlight that in this study we are not interested in the evaluation of chemical reactions between

the oligomeric structures and the gaseous compounds, but only in identifying relevant sites for subsequent adsorption studies.

The CAFIs were calculated in a DFT approach by using the B3LYP exchange-correlation functional and 6-31G basis set on all the atoms, with the aid of the Gaussian 09 computational package [43]. Hirshfeld partition charge method was employed in order to avoid negative CAFI values [44, 45].

Aiming to evaluate the interaction between analytes and PANI derivatives, adsorption studies were carried out for four systems, which were pre-selected from the reactivity study (PANI, PANI-NO_2, PANI-C_6H_5 and PANI-C≡CH). The gaseous chemical species, considered as analytes, were: H_2, H_2S, H_2O, NH_3, and SO_2 [9, 46–48]. In order to simulate the adsorption on the oligomers, these analytes were placed close to the most reactive sites of the derivatives and the resulting structures were then fully optimized in a restricted HF/PM6 approach. Different relative densities ($d_1 = 5$ and $d_2 = 9$ molecules per oligomer) were considered for comparison, and to evaluate possible quantitative effects.

The influence of the analytes on the polymer electronic structure was evaluated via the analysis of average binding energies and changes on the structural features, optical absorption spectra, frontier orbitals distribution, and total density of states in relation to the non-adsorbed systems.

The changes induced on the oligomer geometries were estimated via the calculation of root mean square deviations of the atomic positions (RMSD-AP) considering the isolated oligomers (structures that were fully optimized without the presence of the analytes) in relation to the adsorbed systems, with the aid of VMD and Qmol computational packages [49, 50]. Given the different atoms numbering on the considered structures (isolated and adsorbed systems), only nitrogen atoms were considered for the alignment and RMSD-AP evaluation.

The average binding energies associated with each derivative/analyte system ($\overline{BE}_{PANI-X/Y}$) were estimated from the arithmetic mean of the binding energies evaluated for each relative density (d_1 and d_2) (Eqs. 4 and 5).

$$BE^{(d)}_{PANI-X/Y} = \frac{1}{N^{(d)}}\left[E^{(d)}_{PANI-X/Y} - \left(E^{(d)}_{PANI-X} + E^{(d)}_{Y}\right)\right] \quad (4)$$

$$\overline{BE}_{PANI-X/Y} = \frac{1}{2}\left[BE^{(d1)}_{PANI-X/Y} + BE^{(d2)}_{PANI-X/Y}\right] \quad (5)$$

where N represents the number of analyte molecules (Y) in the system that defines the relative density, d. $E^{(d)}_{PANI-X/Y}$ represents the total energy of the system composed by the derivative PANI-X and N molecules of Y analyte, after optimization. $E^{(d)}_{PANI-X}$ and $E^{(d)}_{Y}$ represent the total energy of the isolated PANI-X derivatives and the distribution of Y analytes, respectively, coming from single-point calculations on the optimized geometries (and spatial distributions) of the adsorbed systems (see Electronic Supplementary Material for details). Since the geometries were optimized in a HF/PM6 approach, the $\overline{BE}_{PANI-X/Y}$ values were estimated via the energies coming from this semiempirical method (and for this reason no correction for BSSE were considered). Indeed, similar approaches have proven to provide reasonable estimation of binding energies in more complex systems [51, 52]. In addition, at the present study we are more interested in a comparative evaluation of the binding energies than obtaining their precise values, so the $\overline{BE}$ values are considered only as qualitative descriptors of the oligomer/analyte interaction.

The theoretical absorption spectra of the systems were calculated in a time-dependent DFT (TD-DFT) approach, employing the B3LYP exchange-correlation functional and 6-31G basis set, with the aid of Gaussian 09 computational package. Five transitions were evaluated, considering only single excitations.

Results and discussion

Derivatives properties

Since most of the proposed derivatives have not been previously synthesized, we have firstly evaluated the influence of the distinct **R** groups on the opto-electronic properties of the compounds in order to guide the search for new promising PANI-based materials for varied applications.

Figure 2 represents the energies of the highest occupied and lowest unoccupied molecular levels (E_{HOMO} and E_{LUMO}) of all the isolated oligomers. The variations observed in the electronic gap (ΔE_{gap}, where $E_{gap} = E_{LUMO} - E_{HOMO}$) in relation to the unmodified PANI are also presented (gray bars).

A reduction on the HOMO energy level is often associated with an improvement on the chemical stability of the compounds [53]. In this context, it can be noticed that the presence of OH, NO_2, C≡CH, and F side groups leads to a significant improvement on the chemical stabilities of the resulting systems, reducing the HOMO level to values around or lower than 5 eV, which is considered an interesting level to hinder the system oxidation [53]. On the other hand, the most prominent changes on the electronic gap are associated with OH, F, and C_6H_5 groups, with larger gaps for R = OH and F and a reduced one for C_6H_5.

Figure 3 presents the HOMO and LUMO spatial distributions on the derivatives structures. Note that the

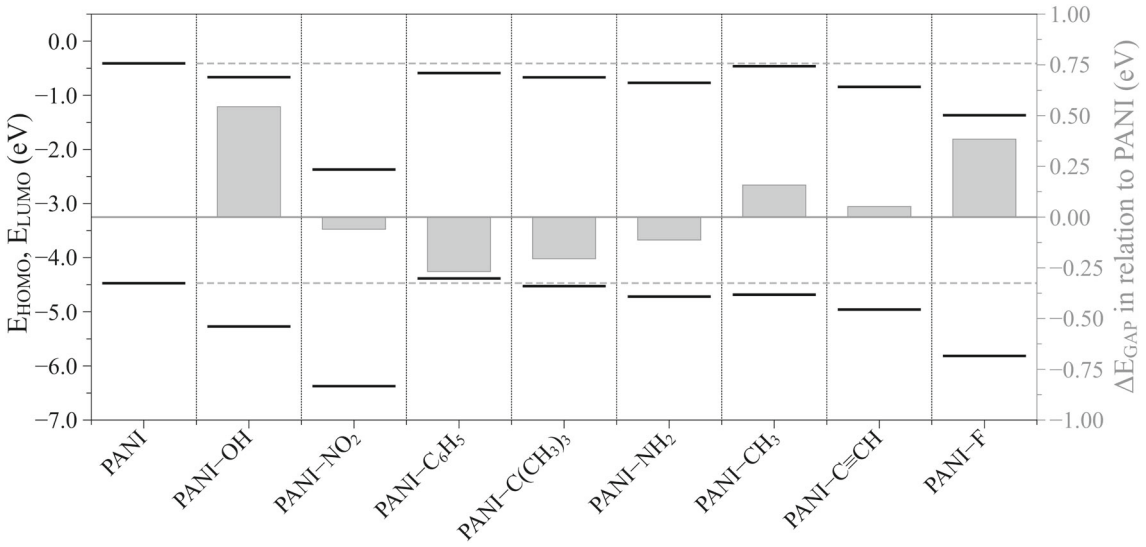

Fig. 2 Changes induced by the presence of the side groups on the frontier energy levels and electronic gap of the N-substituted PANI derivatives

presence of NO_2 and C_6H_5 substituents leads to a significant enhancement on the HOMO-LUMO spatial overlap in relation to the unmodified PANI. In general, such overlap is reduced in the other derivatives.

Figure 4 presents the theoretical absorption spectra of the systems. Note that the obtained main peak position of unmodified oligomer is compatible with the experimental values [34, 54], indicating the plausibility of the methods employed in the description of structural and opto-electronic properties of the oligomers.

As can be noted, the spectra of the derivatives PANI-C_6H_5 and PANI-NO_2 are red shifted in relation to the unmodified PANI, while all the others systems present hypsochromic shifts (blue-shifts). In particular OH and C_6H_5 groups lead to the larger displacements. PANI, PANI-C_6H_5, and PANI-OH derivatives show the more intense relative absorption amplitudes, while very small oscillator strengths are observed for PANI-NH_2, PANI-CH_3, and PANI-$C(CH_3)_3$. Intermediary amplitudes are noticed for PANI-C≡CH, PANI-NO_2, and PANI-F. It is interesting to note that despite of increasing the overall HOMO-LUMO overlap (see Fig. 3), the presence of NO_2 groups does not promote an increase in the relative absorption amplitude, just leading to a red-shift in the spectrum.

In order to evaluate if the opto-electronic properties of the derivatives follow some predictable trend that could guide the synthesis of new compounds, possible correlations between the HOMO and LUMO energy levels, electronic gap ($E_{gap} = E_{LUMO} - E_{HOMO}$), optical gap (first singlet excitation energy), and the Hammet parameters of the **R** groups were evaluated. Figure 5 illustrates the most relevant relationships obtained (see Electronic Supplementary Material for addition evaluations).

From the fittings, it is possible to note a clear dependence of the HOMO and LUMO energy levels with σ_I descriptors. In general, the presence of strong EWGs (by inductive effect - σ_I) leads to significant reductions on HOMO and LUMO energies in a linear and exponential way, respectively. In this sense, at the same time that the attachment of EWGs to the PANI nitrogen lead to more stable systems, it also reduces the electronic gaps, since the changes promoted in E_{LUMO} are larger than those promoted in E_{HOMO}. Some influence of σ_R on the electronic and optical gaps is also observed, however it is not so clear (see Electronic Supplementary Material).

Reactivity studies

Figures 6, 7 and 8 present the results obtained from the CAFI study. Blue and red colors indicate, respectively, the minimum and maximum CAFI values for each derivative. Blue regions are associated with inert sites while red regions indicate the position of the most reactive ones. The other colors represent sites with intermediate reactivities, following the increasing order: blue, green, yellow, orange, and red. Different color scales are defined for each compound.

In general, based on the position of the most reactive sites on the oligomers structures it is possible to define three distinct subgroups:

i. Systems with reduced reactivity (inert oligomers): **R**=$C(CH_3)_3$ and CH_3 (Fig. 6);
ii. Systems with intermediate reactivity: unmodified PANI and PANI-R for **R**=F, OH and NH_2 (Fig. 7);
iii. Systems with high reactivity in more accessible regions: **R**=NO_2, C_6H_5 and C≡CH (Fig. 8).

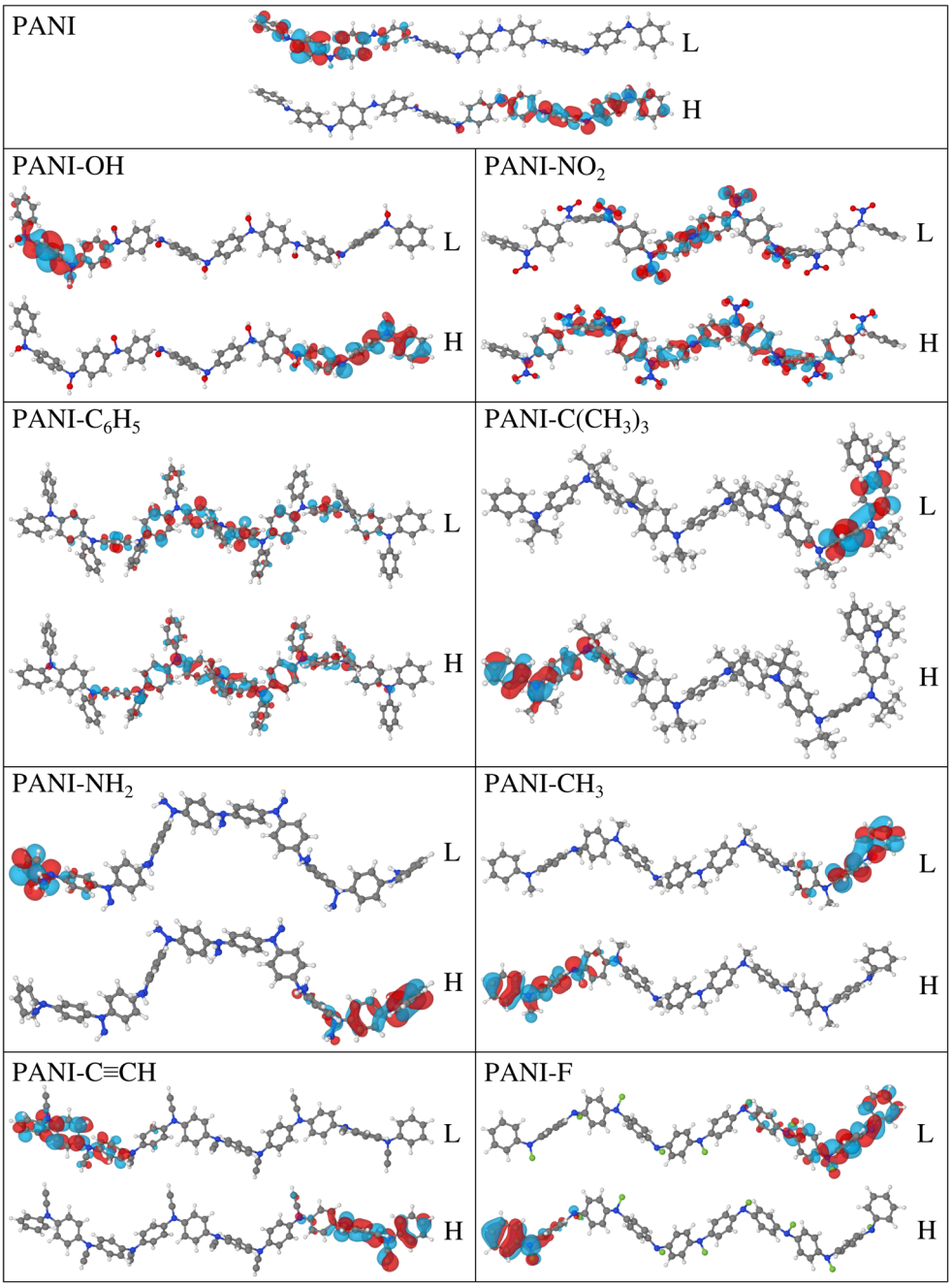

Fig. 3 Spatial distribution of the frontier orbitals on the structure of the N-substituted PANI derivatives. H and L represent, respectively, the HOMO and LUMO

Inert derivatives present higher reactivities on sterically protected sites and/or on the terminal regions of the oligomer structure (a kind of border effect). The intermediate group presents higher reactivities on the central nitrogens and terminal regions, however, reactive sites are also observed on the side branches. Finally, in the third group, the highest reactivities are found on the side ligands. In particular, this last feature is quite interesting for the design of chemical sensors, since these regions are supposed to be more exposed in the polymer-based devices and they can effectively interact with external chemical species (analytes).

The reduced reactivities of CH_3 and $C(CH_3)_3$ based compounds are indeed compatible with experimental studies that indicate the lower susceptibility of N-alkyl PANI derivatives to interact with external chemical species [23, 27].

In order to evaluate if the obtained results follow some trend, the reactivities were analyzed in terms of the Hammet parameters of the employed **R** groups. Figure 9 illustrates

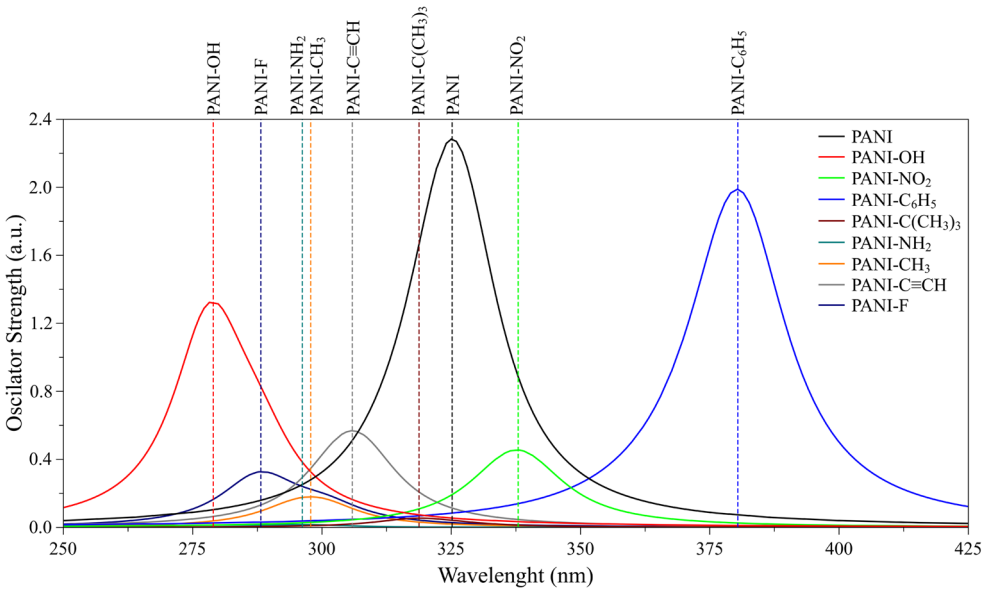

Fig. 4 Spatial distribution of the frontier orbitals on the structure of the N-substituted PANI derivatives. H and L represent, respectively, the HOMO and LUMO

these parameters for all the substituents (Table 1). The most promising groups identified from the CAFIs analyses are highlighted.

Note that the three substituents associated with the most promising derivatives (NO_2, C_6H_5, and C≡CH) are generally classified as inductive EWGs, with a weak resonant effect. Inert systems are associated with ERGs by resonance, with weak polar effect. Finally, intermediate systems are associated with ERGs (by both resonant and polar effects). In this context, we can conclude that, despite the σ_I descriptor being strongly correlated with the opto-electronic properties of the N-substituted PANI derivatives (see Section 1), the most relevant information regarding the reactivity of the systems is associated with the weakness of the resonant effects induced by the **R** groups (small σ_R absolute values). Thus, an appropriated balance between these descriptors is necessary in order to obtain good candidates for N-substituted PANI-based gas sensors.

Adsorption studies

Adsorption studies were carried out only for the most promising systems, that were pre-selected from the reactivity study: PANI-NO_2, PANI-C_6H_5, and PANI-C≡CH. Unmodified PANI was also considered for comparisons.

Since it is known that in some cases structural changes on the polymer conformation can play a relevant role in electrical response of PANI-based systems [9, 55, 56], structural modifications induced by the presence of the chemical species on each one of the derivatives were evaluated. Figure 10 shows the influence of the analytes on the structural properties of the oligomers illustrated by the RMSD-AP values (all the optimized structures are presented in the Electronic Supplementary Material).

For unmodified PANI the presence of the NH_3 and SO_2 species leads to the most significant distortions on the oligomer main chains, no significant modifications are induced by

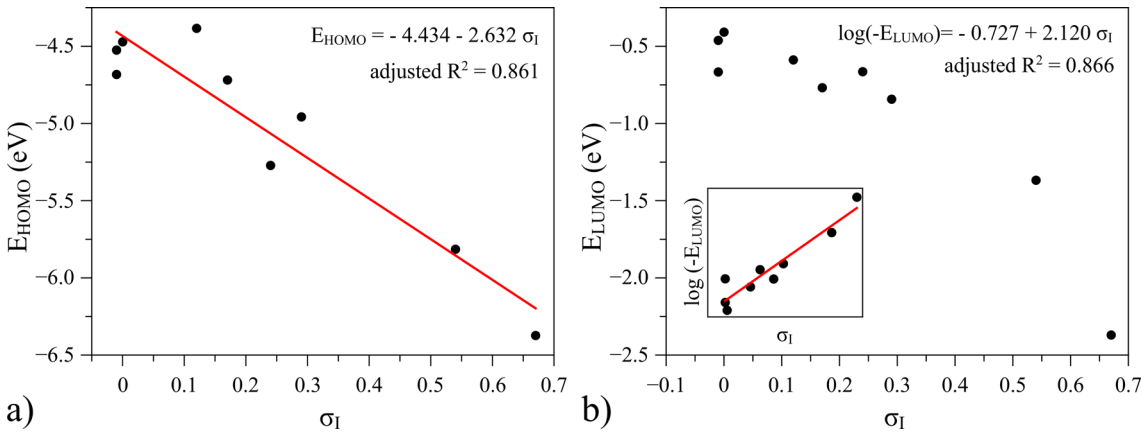

Fig. 5 E_{HOMO} and E_{LUMO} dependence with σ_I Hammet parameters of the **R** groups present in the PANI derivatives

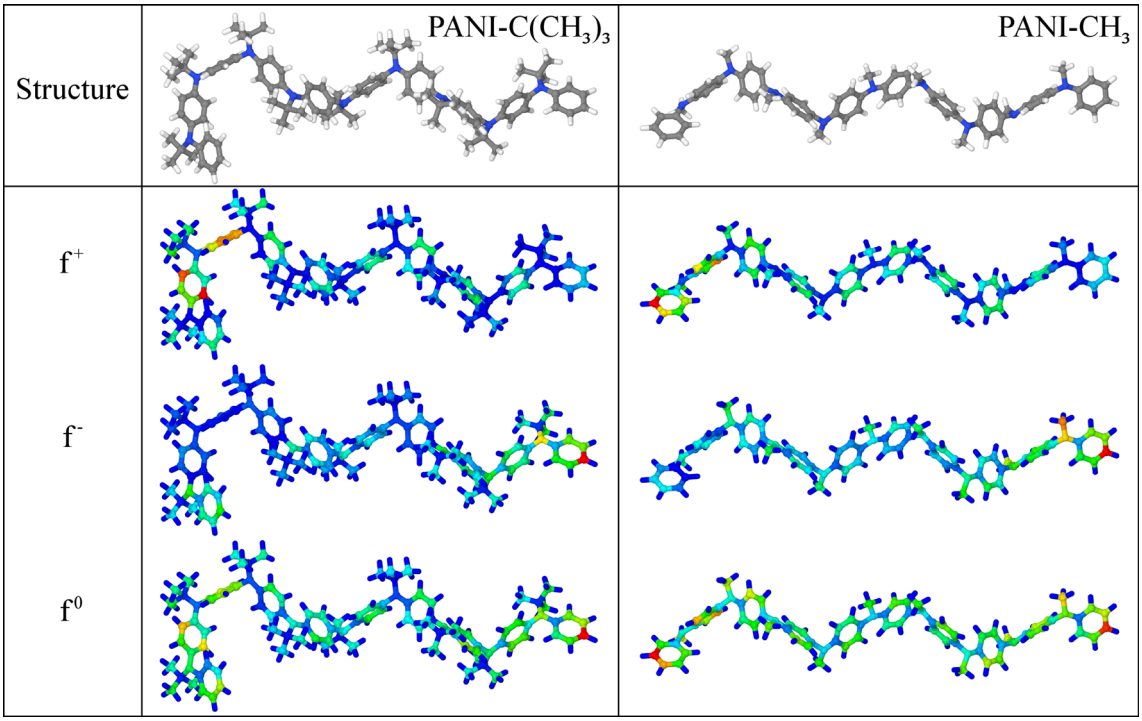

Fig. 6 Color representation of CAFI on the structure of PANI-$C(CH_3)_3$ and PANI-CH_3

the presence of H_2, H_2O and H_2S. For PANI-NO_2, expressive structural distortions are observed for most of the analytes, except for H_2. Finally, constant changes were observed for PANI-C_6H_5 and PANI-C≡CH, independently of the adsorbent molecule, which suggest that the side ramifications of these systems protect the oligomer main chains from the action of the analytes. In addition to the changes presented in Fig. 10, effective interactions between the H_2O oxygen atoms and the side hydrogens of the oligomer derivatives (hydrogen bridges) are also observed, which is a well-known mechanism of interaction between water molecules and doped PANI [57, 58] and is supposed to be less prominent in our non-doped systems.

Figure 11 shows the average binding energies between analytes and derivatives. The error bars define the standard deviations associated with the different densities (for details regarding the calculation of $\overline{BE}_{PANI-X/Y}$ see Electronic Supplementary Material).

As can be noticed, the average analyte/oligomer binding energies vary appreciably in the different systems. For unmodified PANI, the analytes SO_2, H_2O and NH_3 present the highest binding energies (higher than 0.15 eV). This result is compatible with the higher RMSD-AP values obtained for SO_2 and NH_3. On the other hand, the high $\overline{BE}_{PANI/H_2O}$ value suggest that, despite of the low RMSD-AP value associated with these systems, there is an effective interaction between the analytes and the oligomer, probably due to the above-mentioned O–H interactions. Reduced binding energies are also observed in the PANI/H_2S, which is compatible with experimental results that indicates a weak direct interaction between PANI and this analyte [47]. The highest average binding energies are associated with PANI-NO_2 based systems, with $\overline{BE}_{PANI-NO_2/Y} > 0.225eV$, except for H_2 molecules (which is also compatible with the RMSD-AP results). In particular, this derivative presents more significant results than unmodified PANI, which suggests that it could be considered an optimized material for chemical sensors. In general, PANI-C_6H_5 based systems do not exhibit high binding energies, especially in relation to H_2, for which the obtained values are lower than the thermal energy at room temperature. The highest binding energies are associated with H_2O analytes, which can be linked to the effective interaction between these molecules and the side chains of the derivative (see Fig. S4 in the Electronic Supplementary Material). PANI-C≡CH based systems present the less-promising results, with average binding energies lower than $0.10eV$ ($\overline{BE}_{PANI-C\equiv CH/Y} \leqslant 4kT$ at room temperature).

Despite of the interesting results coming from the $\overline{BE}$ analyses, it is important to stress that they must be considered only as qualitative descriptors of the oligomer–analyte interactions, mainly due to the simplified methodology employed in their estimation. Additional evaluations employing long-range, counterpoise and other similar corrections must be employed in order to obtain precise absolute values, however it is not in the scope

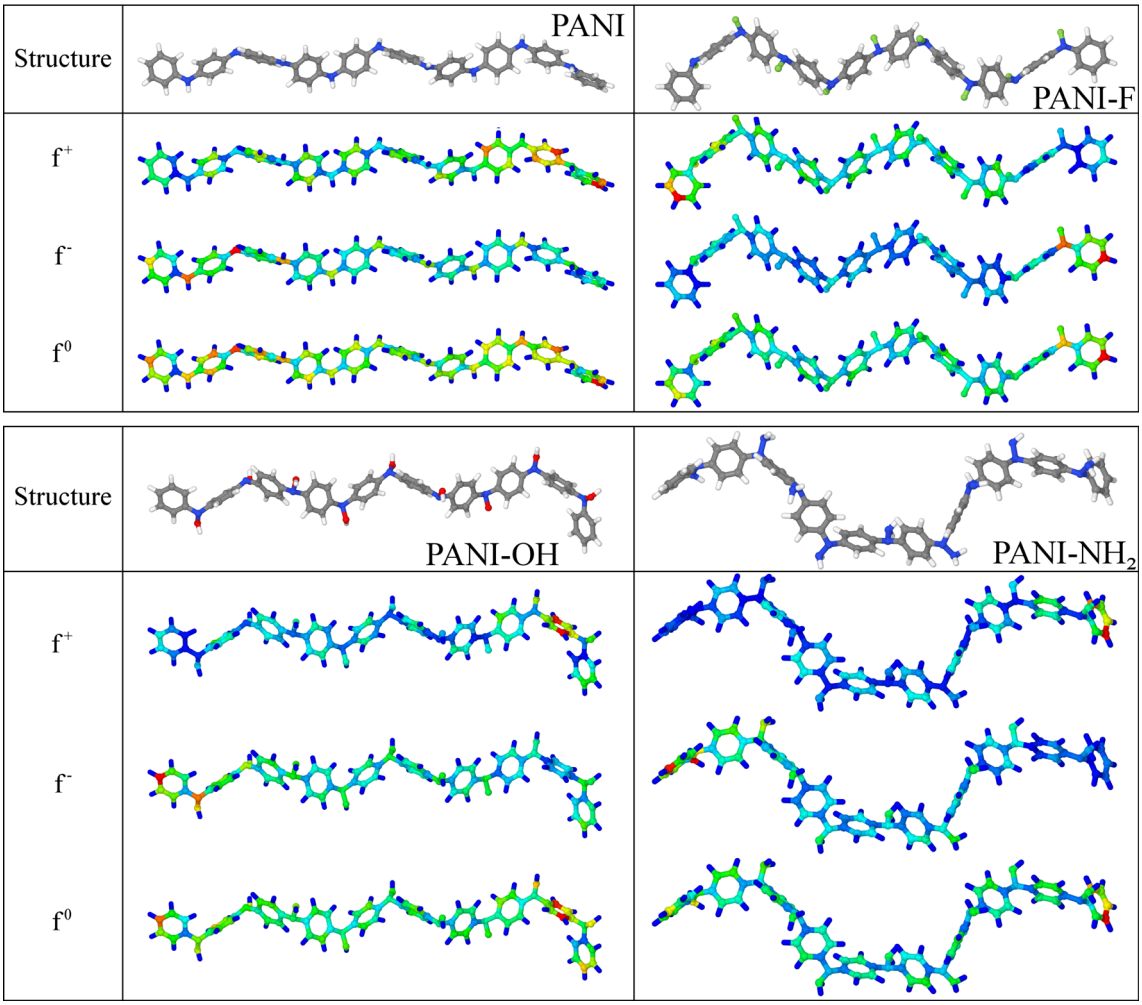

Fig. 7 Color representation of CAFI on the structure of PANI, PANI-F, PANI-OH, and PANI-NH_2

of this report. Nevertheless, it is interesting to highlight that, despite of the simple approach employed to estimate the $\overline{BE}$, the obtained values are still of the same order of magnitude as those estimated via more sophisticated methods, for example for PANI/SO_2 and PANI/NH_3 systems [54, 59].

In order to better identify the changes induced in the electronic structure of the PANI derivatives by the presence of the analytes, the theoretical optical absorption spectra of the systems were evaluated. Figure 12 presents the spectra of isolated oligomers and adsorbed systems with different relative densities (d_1 and d_2). The normalized and non-normalized spectra are presented in order to provide more information regarding the changes induced in the relative positions of the peaks as well as their amplitudes.

For unmodified PANI, a significant red-shift induced by the presence of NH_3 analytes ($\Delta\lambda \sim +16nm$) is observed, which does not depend on the relative density of analytes in the system. This result is in opposition with the effect promoted by NH_3 in positively charged PANI (emeraldine salt) [59], suggesting the existence of a different optical response of leucoemeraldine PANI to the presence of this analyte, which could be explored in more detail experimentally. A small blue-shift is induced by H_2O molecules ($\Delta\lambda \sim -6nm$), with the formation of an small shoulder in d_2. Very intense displacements were observed for the PANI/SO_2 systems (with $\lambda_{max} > 2000nm$) while no significant effects were observed for PANI-H_2 and PANI-H_2S. In general, the main peak shifts are not dependent on the relative densities (d_1 and d_2), suggesting that leucoemeraldine PANI does not present quantitative responses. Regarding the changes observed in the relative amplitudes (oscillator strengths), it is noticed that the systems PANI/H_2O and PANI/H_2S with d_2 density present a significant quenching of the absorption in relation to the non-adsorbed system (and systems with d_1 density),

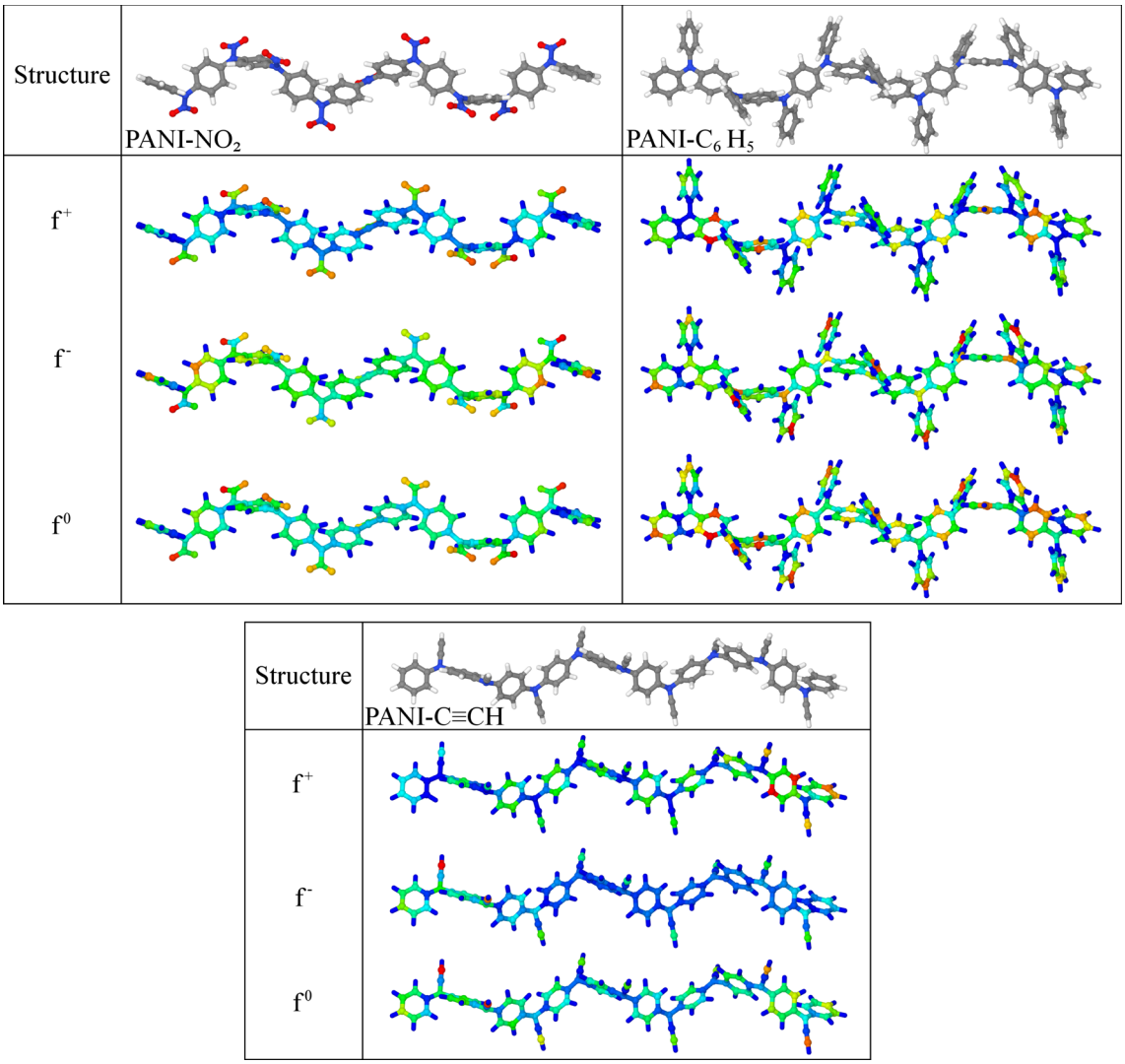

Fig. 8 Color representation of CAFI on the structure of PANI-NO_2, PANI-C_6H_5, and PANI-C≡CH

which suggests a possible quantitative effect. Such feature is also observed in PANI/NH_3 system, however it is not so evident.

For PANI-NO_2, significant changes in the main peak positions are observed for most of the systems, except for PANI-NO_2/H_2. A red shift of about $\sim 5nm$ is observed for PANI-NO_2/H_2S in d_1, while a very significant variation of the spectrum is identified for the higher density, d_2 ($\lambda_{max} \sim 610nm$). It can be attributed to the higher proximity between the oligomer chain and analytes observed in this system after geometry optimization (see Fig. S3 in the Electronic Supplementary Material). A very intense red shift is again observed for SO_2 analytes for both the densities (with $\lambda_{max} > 600nm$). Blue shifts are induced by the presence of NH_3 ($\Delta\lambda \sim -15nm$) and H_2O analytes ($\Delta\lambda \sim -9nm$). Apparently, the main peak displacement in PANI-NO_2/NH_3 system is sensitive to the number of adsorbed species. In addition to the observed shifts, PANI-NO_2/NH_3 and PANI-NO_2/H_2O systems present a quenching in the amplitude of the absorption main peak for higher densities of analytes (d_2).

Analyzing the PANI-C_6H_5-based systems (Fig. 12e–f), it is possible to note that most of the analytes lead to a blue shift in the spectra, followed by a reduction on the amplitude of the main peak. The most prominent effect is induced by the presence of H_2O molecules (green curves), while H_2 analytes (red curves) lead to less significant changes, which are compatible with the results obtained for the binding energies (Fig. 11). Similarly to the other derivatives, the presence of SO_2 molecules leads to a marked change in the main peak position (inset of Fig. 12). In general, the observed responses are sensitive to the number of analytes, with larger effects for higher densities (main peak displacements and amplitudes), with the exception of H_2

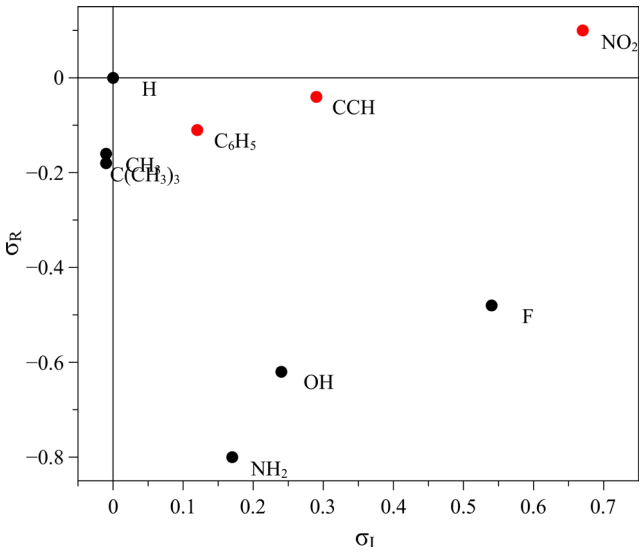

Fig. 9 Representation of Hammet parameters of the **R** groups. Red points define the most promising substituents

and SO_2. Such results indicate the derivative PANI-C_6H_5 as a promising material for quantitative determination of analytes via optical properties.

For PANI-C≡CH, non-predictable changes on the optical properties are observed. In general, it is noticed that H_2S analytes lead to a small blue shift, while NH_3 are associated with red shifts of the absorption main peak. The amplitudes associated with the adsorbed systems are higher than the non-adsorbed ones. There is also no pattern regarding the relative densities.

Based on the results presented above, the following conclusions can be drawn regarding the optical responses of the systems: *i)* unmodified PANI presents interesting (non-quantitative) sensory optical properties with respect to H_2O and NH_3; *ii)* PANI-NO_2 derivative shows quantitative sensory properties regarding H_2O and NH_3, (especially for NH_3); *iii)* PANI-C_6H_5 derivative demonstrates promising sensory properties for all the analytes, especially for H_2O, H_2S and NH_3; *iv)* the PANI-C≡CH derivative presents very anomalous results, with no clear patterns in the optical responses; *v)* all the derivatives show intense changes in the optical responses due to the presence of SO_2 analytes, which are compatible with recently reported theoretical results that indicate PANI-based systems as relevant detectors of SO_x compounds [54].

Aiming to better interpret the changes in the opto-electronic properties of the systems, the effects on the total density of states (DOS) around the frontier levels (HOMO and LUMO) are presented in Fig. 13. The gray regions represent the DOS of isolated oligomers, with the vertical dashed lines illustrating the HOMO and LUMO positions. Dashed and full color lines represent systems with distinct relative densities, d_1 and d_2, respectively.

Regarding unmodified PANI, no visible changes are observed around the energy gap for H_2. Indeed, one of the more accepted mechanism proposed for the interaction between H_2 molecules and PANI is mainly associated with local reactions on charged amine nitrogen sites, which are not present in our undoped PANI model (leucoemeraldine base) [46]. More prominent changes are observed for NH_3 and SO_2 as already identified in the absorption spectra. In particular, the presence of SO_2 molecules leads to the formation of energy levels in the middle of the polymer gap that explains the significant effect on the optical spectra. The results also allow to estimate the influence of the analytes in the electrical response of the undoped PANI based on the changes induced in the frontier levels: *i)* improved transport of intrinsic holes in the presence of H_2O and NH_3, *ii)* improved electron transport properties for H_2S, and *iii)* virtually no gap material for SO_2. Such considerations, however, must be very carefully

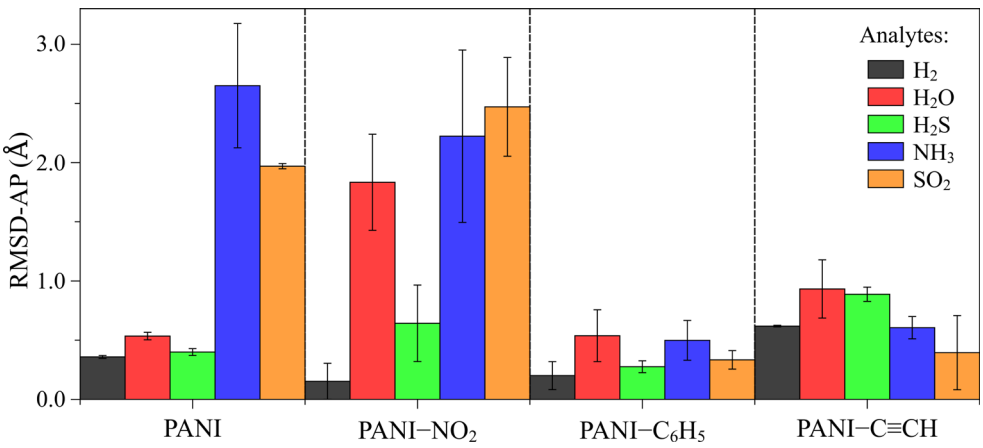

Fig. 10 Average RMSD-AP values for each evaluated system. The error bars represent the standard deviation values coming from the two distinct densities

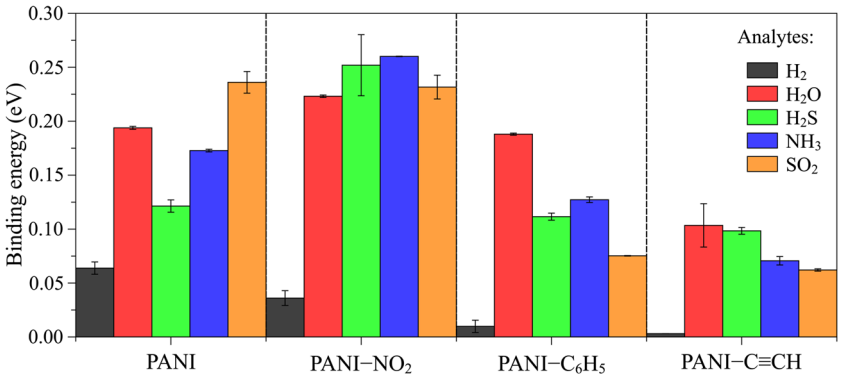

Fig. 11 Average oligomer/analyte binding energy for each evaluated system

evaluated when compared with experimental results, since the electrical response of PANI (our unmodified derivative) is more linked to extrinsic charge carriers (coming from varied doping mechanisms) than intrinsic ones. This effect is evident for PANI/NH_3 systems, which present a reduced conductivity induced by PANI deprotonation [46, 48] and PANI/H_2S, which electrical response depends on the functionalization/substrate employed [9, 47, 48, 60]. Nevertheless, given the absence of the typical salt/base transitions, this dependence must be reduced in our N-substituted derivatives.

Similarly to unmodified PANI, PANI-NO_2 presents no visible changes induced by the presence H_2 analytes. The most significant modifications are observed for H_2O, NH_3, and SO_2. It is possible to note that for H_2O and NH_3 species the changes on the optical spectra are associated with (a density dependent) change on the LUMO levels. The presence of SO_2 molecules also promotes the formation of new levels in the middle of the gap. Regarding the electrical response of the systems, it is expected a reduced electronic transport for PANI-NO_2 derivatives exposed to H_2O and NH_3, and a strong influence of electron-trap mechanisms in polymers exposed to SO_2. The anomalous result observed in PANI-NO_2/$H_2S(d_2)$ system can be associated with an oligomer-analyte chemical bond generated after geometry optimization (see Fig. S3 in the Electronic Supplementary Material).

Very subtle variations are observed in PANI-C_6H_5-based systems, however, since these changes are mainly associated with the frontier orbitals, they lead to quantitative displacements in the absorption main peaks. It is more evident for H_2S and H_2O, where more significant changes are observed around the LUMO level. Similar effects are noticed for PANI-C≡CH in relation to H_2O and NH_3: increase in the energy of HOMO and LUMO levels. Changes in the LUMO (energy decrease) are noticed for H_2S and SO_2 and no significant changes are observed for H_2. In particular, the formation of new levels in the polymer gap are again observed for SO_2.

In general, most of the above-discussed changes in the total DOS are linked to small modifications on the spatial distribution of the HOMO and LUMO on the structure of the adsorbed systems, presented in the Electronic Supplementary Material. In general, only slight changes regarding the isolated systems are observed with an interesting exception for SO_2. For this analyte, the new LUMOs are located on the gaseous compounds instead of on the oligomers, suggesting that despite of promoting significant changes in the electronic gaps, the charge transport in these systems must be dominated by hopping processes between localized states instead of band-like charge transport mechanisms.

Finally, based on the results presented in this report, it is possible to summarize that all the systems present no responses for H_2 while the most significant changes on the opto-electronic properties are linked to SO_2. Specially, the results obtained for SO_2 are quite compatible with those reported by Shokuhi Rad and collaborators [54], which indicate the existence of significant sensory properties of PANI-based oligomers in relation to these analytes. Our data reinforce this observation, suggesting that N-substituted derivatives can also be employed for the detection of such compounds. Our results also point out the plausibility of the detection of H_2S, H_2O and NH_3 molecules via unmodified and N-substituted PANI derivatives as already proposed in the literature for functionalized, doped and nanostructured PANI [8–11]. In particular, the most promising results are observed for PANI-NO_2 and PANI-C_6H_5 in relation to the electrical and optical responses, respectively, which indicate these materials as interesting candidates for the development of improved PANI-based chemical sensors.

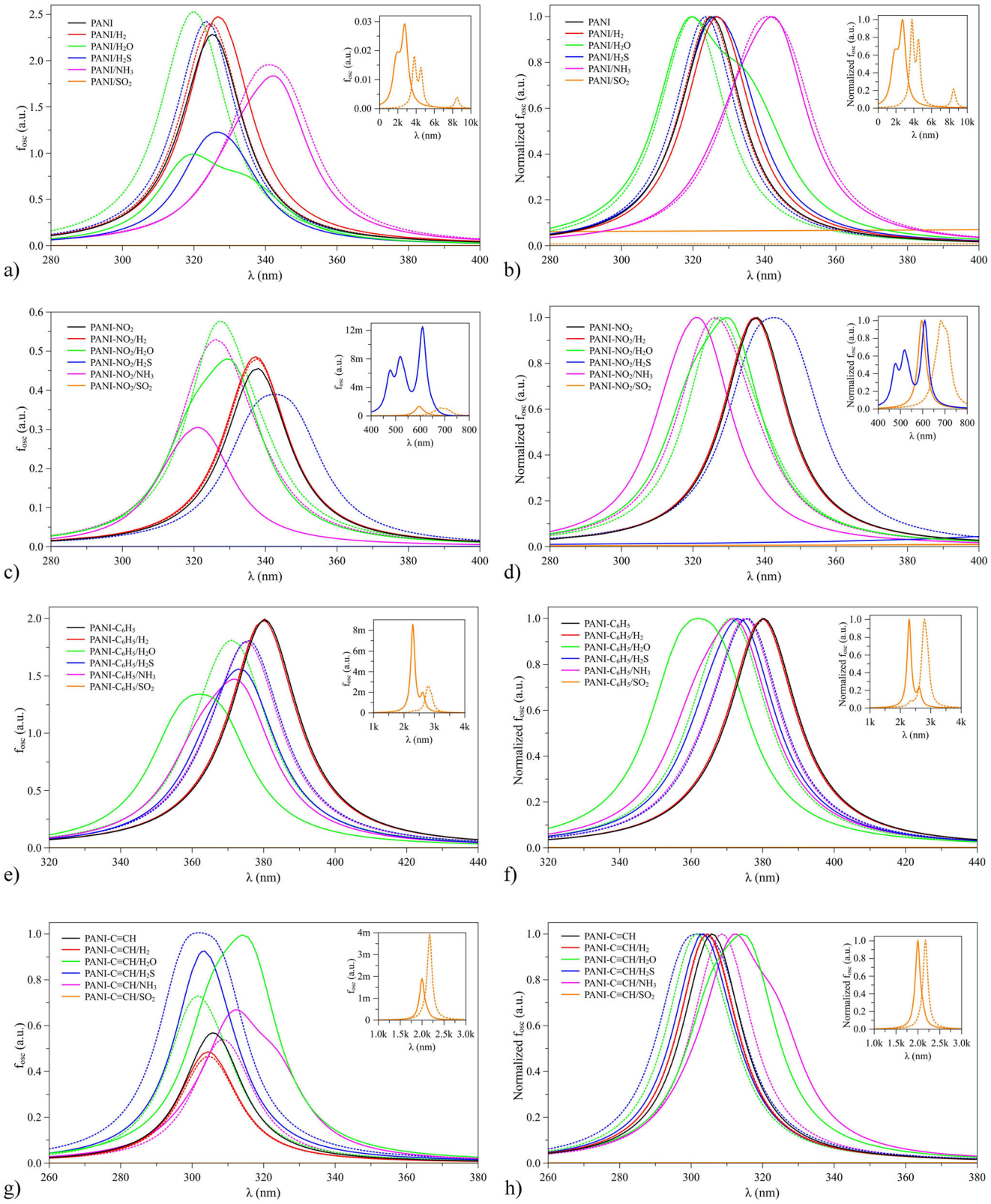

Fig. 12 Non-normalized and normalized absorption spectra of PANI (**a**, **b**), PANI-NO_2 (**c**, **d**), PANI-C_6H_5 (**e**, **f**), and PANI-C≡CH (**g**, **h**) before and after the adsorption of distinct analytes at the densities d_1 (dotted lines) and d_2 (full lines)

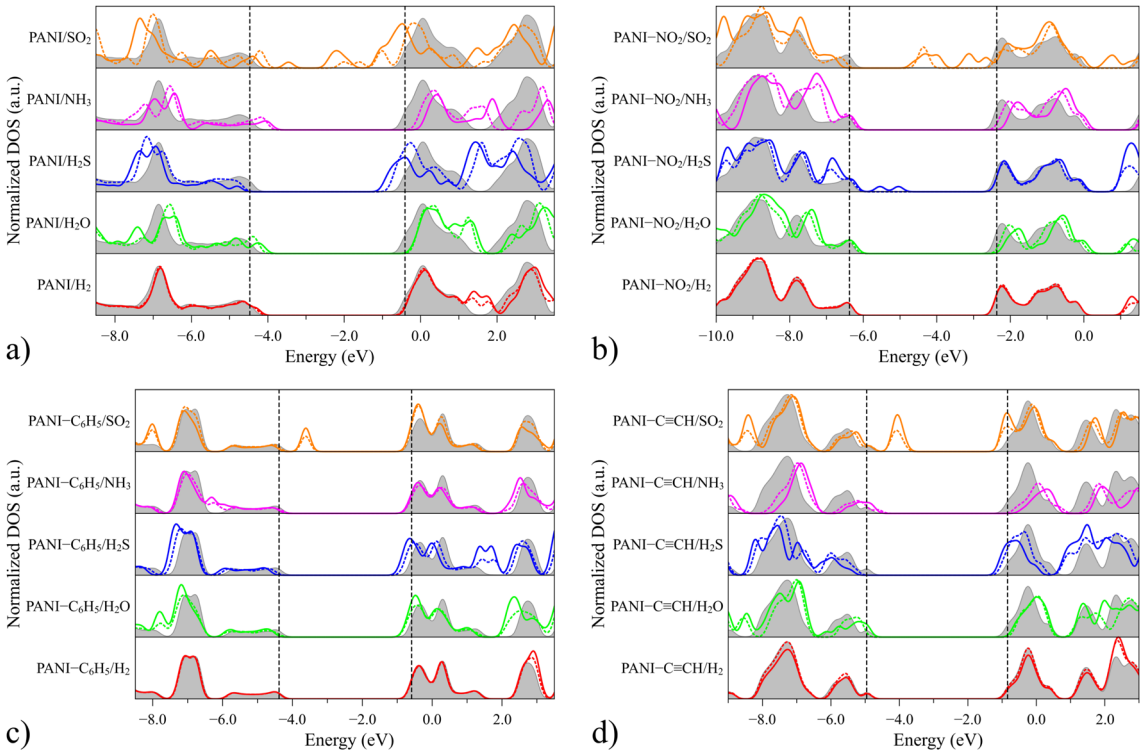

Fig. 13 Normalized DOS for **a** PANI, **b** PANI-NO_2, **c** PANI-C_6H_5, and **d** PANI-C≡CH systems at densities d_1 (dotted lines) and d_2 (full lines) for different analytes. The gray shadows represent the DOS of isolated systems for comparison

Conclusions

In the present work, we have evaluated the local reactivities and the influence of adsorbent species on the electronic structure of N-substituted PANI derivatives for applications in chemical sensors.

The analysis of the influence the **R** groups on the opto-electronic properties of the derivatives indicates that the use of EWGs attached to the PANI nitrogen leads to materials with improved chemical stabilities and lower electronic gaps. It was also shown that other properties of interest can also be adjusted by an appropriated choice of the side N-substituents by considering the inductive and resonant Hammet parameters.

The reactivity study indicates that the incorporation of specific ramifications can lead to significant changes in the spatial distribution of the most reactive sites on the polymer chain, leading to possible improvements on the sensory properties of the resulting systems. Specially, the results show that the attachment of inductive EWGs with weak resonant effects into the PANI structures leads to derivatives with higher reactivities on more accessible side branches, which is an interesting feature for the application of polymeric systems in active layers of chemical sensors.

Finally, adsorption studies were carried out for the most promising derivatives. The compounds PANI-NO_2 and PANI-C_6H_5 presented the most significant (and quantitative) changes on the electronic and optical properties induced by varied adsorbents. In particular PANI-NO_2 has presented the highest average binding energies, while PANI-C_6H_5 showed the most promising optical responses. All the evaluated systems presented high sensitivity to SO_2 species and very low sensory properties in relation to H_2.

Acknowledgements The authors thank the Brazilian agencies FAPESP (Proc. 2016/05954-0) and CNPq (Proc. 448310/2014-7) for the financial support. This research was also supported by resources supplied by the Center for Scientific Computing (NCC/GridUNESP) of the São Paulo State University (UNESP).

References

1. Baraton MI, Organization NAT (eds) (2009) Sensors for environment, health and security: advanced materials and technologies. NATO science for peace and security series. Series C, Environmental security. Springer, Dordrecht
2. Liu X, Cheng S, Liu H, Hu S, Zhang D, Ning H (2012) Sensors 12(12):9635. https://doi.org/10.3390/s120709635
3. Adhikari B, Majumdar S (2004) Prog Polym Sci 29(7):699. https://doi.org/10.1016/j.progpolymsci.2004.03.002
4. Jin Z, Su Y, Duan Y (2001) Sensors Actuators B Chem 72(1):75. https://doi.org/10.1016/S0925-4005(00)00636-5
5. Haynes A, Gouma PI (2009). In: Baraton M. I. (ed) Sensors for Environment, Health and Security. Springer, Netherlands, pp 451–459

6. Crowley K, Smyth MR, Killard AJ, Morrin A (2012) Chem Pap 67(8):771. https://doi.org/10.2478/s11696-012-0301-9
7. Wu Z, Chen X, Zhu S, Zhou Z, Yao Y, Quan W, Liu B (2013) Sensors Actuators B Chem 178:485. https://doi.org/10.1016/j.snb.2013.01.014
8. Sengupta PP, Barik S, Adhikari B (2006) Mater Manuf Process 21(3):263. https://doi.org/10.1080/10426910500464602
9. Fratoddi I, Venditti I, Cametti C, Russo MV (2015) Sensors Actuators B Chem 220:534. https://doi.org/10.1016/j.snb.2015.05.107
10. Crowley K, Morrin A, Shepherd RL, in het Panhuis M, Wallace GG, Smyth MR, Killard AJ (2010) IEEE Sensors J 10(9):1419. https://doi.org/10.1109/JSEN.2010.2044996
11. Pawar SG, Chougule MA, Sen S, Patil VB (2012) J Appl Polym Sci 125(2):1418. https://doi.org/10.1002/app.35468
12. Syed AA, Dinesan MK (1991) Talanta 38(8):815. https://doi.org/10.1016/0039-9140(91)80261-W
13. Stejskal J, Sapurina I, Trchová M (2010) Prog Polym Sci 35(12):1420. https://doi.org/10.1016/j.progpolymsci.2010.07.006
14. Tousek J, Tousková J, Chomutová R, Krivka I, Hajná M, Stejskal J (2017) Synth Met 234:161. https://doi.org/10.1016/j.synthmet.2017.10.015
15. Bhadra S, Khastgir D, Singha NK, Lee JH (2009) Prog Polym Sci 34(8):783. https://doi.org/10.1016/j.progpolymsci.2009.04.003
16. Boeva ZA, Sergeyev VG (2014) Polym Sci Ser C 56(1):144. https://doi.org/10.1134/S1811238214010032
17. D'Aprano G, Leclerc M, Zotti G, Schiavon G (1995) Chem Mater 7(1):33. https://doi.org/10.1021/cm00049a008
18. Bavastrello V, Correia Terencio TB, Nicolini C (2011) Polymer 52(1):46. https://doi.org/10.1016/j.polymer.2010.10.022
19. Jaymand M (2013) Prog Polym Sci 38(9):1287. https://doi.org/10.1016/j.progpolymsci.2013.05.015
20. Manohar S, Macdiarmid A, Cromack K, Ginder J, Epstein A (1989) Synth Met 29(1):349. https://doi.org/10.1016/0379-6779(89)90317-2
21. Langer JJ (1990) Synth Met 35(3):295. https://doi.org/10.1016/0379-6779(90)90213-5
22. Chevalier JW, Bergeron JY, Dao LH (1992) Macromolecules 25(13):3325. https://doi.org/10.1021/ma00039a001
23. Lindfors T, Ivaska A (2002) J Electroanal Chem 531(1):43. https://doi.org/10.1016/S0022-0728(02)01005-7
24. Gheybi H, Abbasian M, Moghaddam PN, Entezami AA (2007) J Appl Polym Sci 106(5):3495. https://doi.org/10.1002/app.27037
25. Gheybi H, Bagheri M, Alizadeh Z, Entezami AA (2008) Polym Adv Technol 19(8):967. https://doi.org/10.1002/pat.1062
26. Tarassi M, Zadehnazari A (2016) J Chil Chem Soc 61(3):3108. https://doi.org/10.4067/S0717-97072016000300020
27. Lindfors T, Ivaska A (2002) J Electroanal Chem 535(1-2):65. https://doi.org/10.1016/S0022-0728(02)01172-5
28. Huang X, McVerry BT, Marambio-Jones C, Wong MCY, Hoek EMV, Kaner RB (2015) J Mater Chem A 3(16):8725. https://doi.org/10.1039/C5TA00900F
29. Cataldo F, Maltese P (2002) Eur Polym J 38(9):1791. https://doi.org/10.1016/S0014-3057(02)00070-8
30. Carey FA, Sundberg RJ (2007) Advanced organic chemistry: Part A: Structure and mechanisms. Springer Science & Business Media, Berlin
31. Stewart JJP (2007) J Mol Model 13(12):1173. https://doi.org/10.1007/s00894-007-0233-4
32. Stewart JJP (1990) J Comput Aided Mol Des 4(1):1. https://doi.org/10.1007/BF00128336
33. Stewart JJP (2016) MOPAC2016: Molecular orbital package. http://openmopac.net
34. de Oliveira ZT, dos Santos M (2000) Chem Phys 260(1-2):95. https://doi.org/10.1016/S0301-0104(00)00209-3
35. Batagin-Neto A, Oliveira EF, Graeff CF, Lavarda FC (2013) Mol Simul 39(4):309. https://doi.org/10.1080/08927022.2012.724174
36. Oliveira EF, Lavarda FC (2017) Mol Simul 43(18):1496. https://doi.org/10.1080/08927022.2017.1321759
37. Yang W, Mortier WJ (1986) J Am Chem Soc 108(19):5708. https://doi.org/10.1021/ja00279a008
38. Mineva. T (2006) Journal of Molecular Structure: THEOCHEM 762(1-3). https://doi.org/10.1016/j.theochem.2005.08.044
39. Bronze-Uhle ES, Batagin-Neto A, Lavarda FC, Graeff CFO (2011) J Appl Phys 110(7):073510. https://doi.org/10.1063/1.3644946
40. Batagin-Neto A, Bronze-Uhle E, Vismara M, Assis A, Castro F, Geiger T, Lavarda F, Graeff C (2013) Current Phys Chem 3(4):431. https://doi.org/10.2174/18779468113036660026
41. Cesarino I, Simões R. P., Lavarda FC, Batagin-Neto A (2016) Electrochim Acta 192:8. https://doi.org/10.1016/j.electacta.2016.01.178
42. Martins LM, Vieira SF, Baldacim GB, Bregadiolli BA, Caraschi JC, Batagin-Neto A, Silva-Filho LC (2018) Dyes Pigments 148:81. https://doi.org/10.1016/j.dyepig.2017.08.056
43. Frisch MJ, Trucks GW, Schlegel HB, Scuseria GE, Robb MA, Cheeseman JR, Scalmani G, Barone V, Mennucci B, Petersson GA, Nakatsuji H (2009) Gaussian 09
44. Roy RK, Pal S, Hirao K (1999) J Chem Phys 110(17):8236. https://doi.org/10.1063/1.478792
45. de Proft F, Van Alsenoy C, Peeters A, Langenaeker W, Geerlings P (2002) J Comput Chem 23(12):1198. https://doi.org/10.1002/jcc.10067
46. Virji S, Kaner RB, Weiller BH (2006) J Phys Chem B 110(44):22266. https://doi.org/10.1021/jp063166g
47. Shirsat MD, Bangar MA, Deshusses MA, Myung NV, Mulchandani A (2009) Appl Phys Lett 94(8):083502. https://doi.org/10.1063/1.3070237
48. Lim JH, Phiboolsirichit N, Mubeen S, Deshusses MA, Mulchandani A, Myung NV (2010) Nanotechnology 21(7):075502. https://doi.org/10.1088/0957-4484/21/7/075502
49. Humphrey W, Dalke A, Schulten K (1996) J Mol Graph 14(1):33. https://doi.org/10.1016/0263-7855(96)00018-5
50. Gans JD, Shalloway D (2001) J Mol Graph Model 19(6):557. https://doi.org/10.1016/S1093-3263(01)00090-0
51. Vincent MA, Hillier IH (2014) J Chem Inf Model 54(8):2255. https://doi.org/10.1021/ci5003729
52. Daniel CRA, Rodrigues NM, da Costa NB, Freire RO (2015) J Phys Chem C 119(41):23398. https://doi.org/10.1021/acs.jpcc.5b05599
53. Takimiya K, Osaka I, Nakano M (2014) Chem Mater 26(1):587. https://doi.org/10.1021/cm4021063
54. Shokuhi Rad A, Ghasemi Ateni S, Tayebi HA, Valipour P, Pouralijan Foukolaei V (2016) Journal of Sulfur Chemistry, 1–10. https://doi.org/10.1080/17415993.2016.1170834
55. Yang LY, Liau WB (2009) Mater Chem Phys 115(1):28. https://doi.org/10.1016/j.matchemphys.2008.10.074
56. Liu SS, Bian LJ, Luan F, Sun MT, Liu XX (2012) Synth Met 162(9-10):862. https://doi.org/10.1016/j.synthmet.2012.03.015
57. Timofeeva O, Lubentsov B, Sudakova Y, Chernyshov D, Khidekel' M. (1991) Synth Met 40(1):111. https://doi.org/10.1016/0379-6779(91)91493-T
58. Lubentsov B, Timofeeva O, Khidekel' M. (1991) Synth Met 45(2):235. https://doi.org/10.1016/0379-6779(91)91808-N
59. Ullah H, Shah AHA, Bilal S, Ayub K (2013) J Phys Chem C 117(45):23701. https://doi.org/10.1021/jp407132c
60. Mekki A, Joshi N, Singh A, Salmi Z, Jha P, Decorse P, Lau-Truong S, Mahmoud R, Chehimi MM, Aswal DK, Gupta SK (2014) Org Electron 15(1):71. https://doi.org/10.1016/j.orgel.2013.10.012